U.S. Department of Energy: Research Grant

Final Technical Report

Award Number: SC0010579

Institution: Northern Arizona University

Project Title: "Multiple element isotope probes, NanoSIMS, and the functional genomics of microbial carbon cycling in soils in response to chronic climatic change."

Project Period: 09/01/2013 – 08/31/2017

Principal Investigator: Bruce A. Hungate

U.S. Department of Energy: Research Grant Progress Report

Title of Project: Multiple element isotope probes, NanoSIMS, and the functional genomics of microbial carbon cycling in soils in response to chronic climatic change

Funding Opportunity FOA Number: DE-FOA0000866

DOE/Office of Science Program Office: Biological & Environmental Research

Grant Number: DE-SC0010579

Principal Investigator: Bruce A. Hungate
928 523 0925
Bruce.Hungate@nau.edu

Institution: Northern Arizona University
Office of Grants and Contract Services
Northern Arizona University
1298 South Knoles Drive, Room #240
Flagstaff AZ 86011
Phone: 928-523-4880
Fax: 928-523-1075

Date Submitted: 24 March 2018

National Laboratory Partner: Lawrence Livermore National Laboratory

---

Project Results:

Summary:

In this project, we developed an innovative and ground-breaking technique, quantitative stable isotope probing, a technique that uses density separation of nucleic acids as a quantitative measurement technique. This work is substantial because it advances SIP beyond the qualitative technique that has dominate the field for years. The first methods paper was published in Applied and Environmental Microbiology (Hungate et al. 2015), and this paper describes the mathematical model underlying the quantitative interpretation. A second methods paper (Schwartz et al. 2015) provides a conceptual overview of the method and its application to research problems. A third methods paper was just published (Koch et al. 2018), in which we develop the quantitative model combining sequencing and isotope data to estimate actual rates of microbial growth and death in natural populations. This work has met much enthusiasm in scientific presentations around the world. It has met with equally enthusiastic resistance in the peer-review process, though our record of publication to date argues that people are accepting the merits of the approach. The skepticism and resistance are also potentially signs that this technique is pushing the field forward, albeit with some of the discomfort that accompanies extrapolation. Part of this is a cultural element in the

field – the field of microbiology is not accustomed to the assumptions of ecosystem science. Research conducted in this project has pushed the philosophical perspective that major advances can occur when we advocate a sound merger between the traditions of strong inference in microbiology with those of grounded scaling in ecosystem science.

We also made important technical advances in the detection of multiple isotopes in microbial samples using Nano-SIMS. This includes the simultaneous detection of ^{18}O, ^{13}C, and ^{15}N in whole microbial cells and in nanogram quantities of bulk nucleic acids extracted from environmental samples. This powerful approach provides a measure of microbial activities in complex mixed communities and can also be used to screen samples before SIP processing. Additionally, we made significant improvements in our Chip-SIP pipeline, better facilitating the application of multiple isotope tracing experiments in environmental samples to study taxon specific substrate consumption patterns, thus improving our ability to make direct links between active microbes and processes of interest.

Detailed description of results and their implications

1) *Quantitative Stable Isotope Probing*

A. ***New Method Developed*** The basic model uses sequence recovery in density fractions to calculate isotopic composition of individual taxa or gene sequences. In brief, this is significant for ecology and biogeochemistry, because the isotope composition of biomarkers is the springboard for quantitative assessment of the imprint of biodiversity on ecosystems, including carbon cycling. The text below provides more detail on this development and its application.

Summary: Microorganisms grow and transform elements at different rates, yet quantifying this variation among microbial taxa in intact communities remains a pressing challenge in microbial ecology. In this work, we further developed quantitative stable isotope probing (qSIP), which combines isopycnic separation of nucleic acids, quantitative polymerase chain reaction, and sequencing to determine the isotopic composition of DNA from individual bacterial taxa after exposure to isotope tracers. In contrast to standard stable isotope probing (SIP), where the researcher selects which density fractions to sequence after isopycnic separation, in qSIP all fractions are sequenced individually. The average density across all fractions in which an individual taxon was recovered, weighted by abundance, yields an average density of DNA for each taxon, proportional to its isotopic composition. This approach isolates the influence of isotope tracer incorporation on the density of DNA from the influence of nucleic acid composition (guanine plus cytosine content), which varies among taxa and can confound interpretation of SIP experiments. In soil incubations, exposure to ^{18}O-H_2O or ^{13}C-glucose caused significant variation among bacterial taxa in ^{18}O or ^{13}C composition. Addition of glucose increased assimilation of ^{18}O into DNA from ^{18}O-H_2O, though the increase in ^{18}O composition was greater than changes in ^{13}C composition after ^{13}C-glucose amendment would predict. This indicates glucose addition indirectly stimulated microorganisms to use other substrates for growth. Our approach can identify biogeochemically significant taxa in the microbial community and quantify their contributions to element transformations and ecosystem processes.

Despite tremendous progress applying molecular tools to understand microbial diversity of intact communities (Muyzer *et al.*, 1993; Amann *et al.*, 1995; Roesch *et al.*, 2007), our understanding of how individual microbial taxa contribute quantitatively to element cycling remains weak. Stable

isotope probing (SIP) partly addresses this challenge, in that it links physically the fluxes of elements to an organism's genome. In typical SIP applications, organisms that utilize isotopically-labeled compounds incorporate the heavy isotope into their nucleic acids, which can be separated by density centrifugation from nucleic acids of organisms that did not utilize the labeled substrates (Radajewski *et al.*, 2000). Centrifugation yields a continuous distribution of nucleic acids along a density gradient, with greater separation for the labeled compared to the unlabeled samples (Radajewski *et al.*, 2000; Buckley *et al.*, 2007). The common practice is then to use a **qualitative** approach, selecting density ranges that distinguish "labeled" from "unlabeled" nucleic acid bands, sequencing them, and interpreting the "labeled" range to contain nucleic acids from organisms that utilized the labeled substrate for growth (Hutchens *et al.*, 2004; Mau *et al.*, 2014; Schwartz *et al.*, 2014; Sharp *et al.*, 2014). Often, the selected ranges focus on discrete density intervals representing "heavy" and "light" fractions, excluding analysis of DNA at intermediate densities (Aanderud *et al.*, 2015; Schmidt *et al.*, 2015). However, GC content also influences the density of DNA (Schildkraut, 1962), so traditional stable isotope probing may confound isotope incorporation with natural variation in GC content. In some cases, only the "heavy" fractions in both labeled and unlabeled treatments are sequenced and compared: any new organisms that appear in the heavy fraction of the labeled treatment are inferred to have taken up enough of the isotope tracer to have significantly shifted the density of their DNA (Jayamani & Cupples, 2015). Thus, SIP as practiced traditionally can identify organisms utilizing a particular substrate, but the selection of density fractions can result in incomplete taxonomic coverage, and **the biogeochemical inferences supported by this approach are qualitative**. Traditional SIP does not quantify isotopic incorporation, the first step in determining the rate of substrate utilization, and the foundation for comparing rates of substrate utilization among different taxa. Stable isotopes are powerful tools for quantifying rates of element fluxes into and through organisms (Peterson & Fry, 1987; Schimel, 1993). Extracting quantitative information about the isotopic composition of nucleic acids in stable isotope probing experiments would substantially advance the technique in its application to quantitative microbial biogeochemistry. In our work, we overcome this limitation by demonstrating how stable isotope probing can quantitative in that density separation yields quantitative estimates of isotope incorporation into individual bacterial taxa.

Method for Calculating Isotope Tracer Incorporation

Our experimental scheme, from soil collection, incubation, through to nucleic acid extraction and analysis is summarized in Figure 1 and described in more detail in the published manuscript (Hungate et al. 2014, Applied and Environmental Microbiology, doi:10.1128/AEM.02280-15). Soil (0-15 cm) was collected in November 2012 from a ponderosa pine forest meadow, located on the C. Hart Merriam Elevation Gradient in Northern Arizona, USA (35.42N, -111.67W, http://www.mpcer.nau.edu/gradient). Laboratory incubations with isotope additions were then conducted as described in the published manuscript. After the isotope addition experiment and DNA extraction, for each of bacterial taxon sequenced, we calculated the average density of that taxon's extracted DNA by weighting the density of each fraction by the proportional abundance of its 16S rRNA sequence. We then computed the difference in weighted-average densities between the heavy and light isotope addition for oxygen and carbon comparisons (^{18}O-H_2O vs. natural abundance H_2O, ^{13}C-glucose vs. natural abundance glucose) for each taxon in both the reference and added glucose treatments. Using those taxon-specific differences in weighted-

average density, we modeled the excess atom fraction (^{18}O and ^{13}C) in the 16S rRNA gene sequence of each taxon. Model assumptions and calculations for all variables are described in

Figure 1. Conceptual model of the quantitative stable isotope probing technique, from sample collection to determining the density of 16S rRNA gene fractions for individual taxa and their corresponding values of atom % stable isotope composition. Note: except for the addition of the stable isotope tracer at the beginning of the incubation, all steps are applied identically to both labeled and unlabeled samples. Artwork by Victor Leshyk.

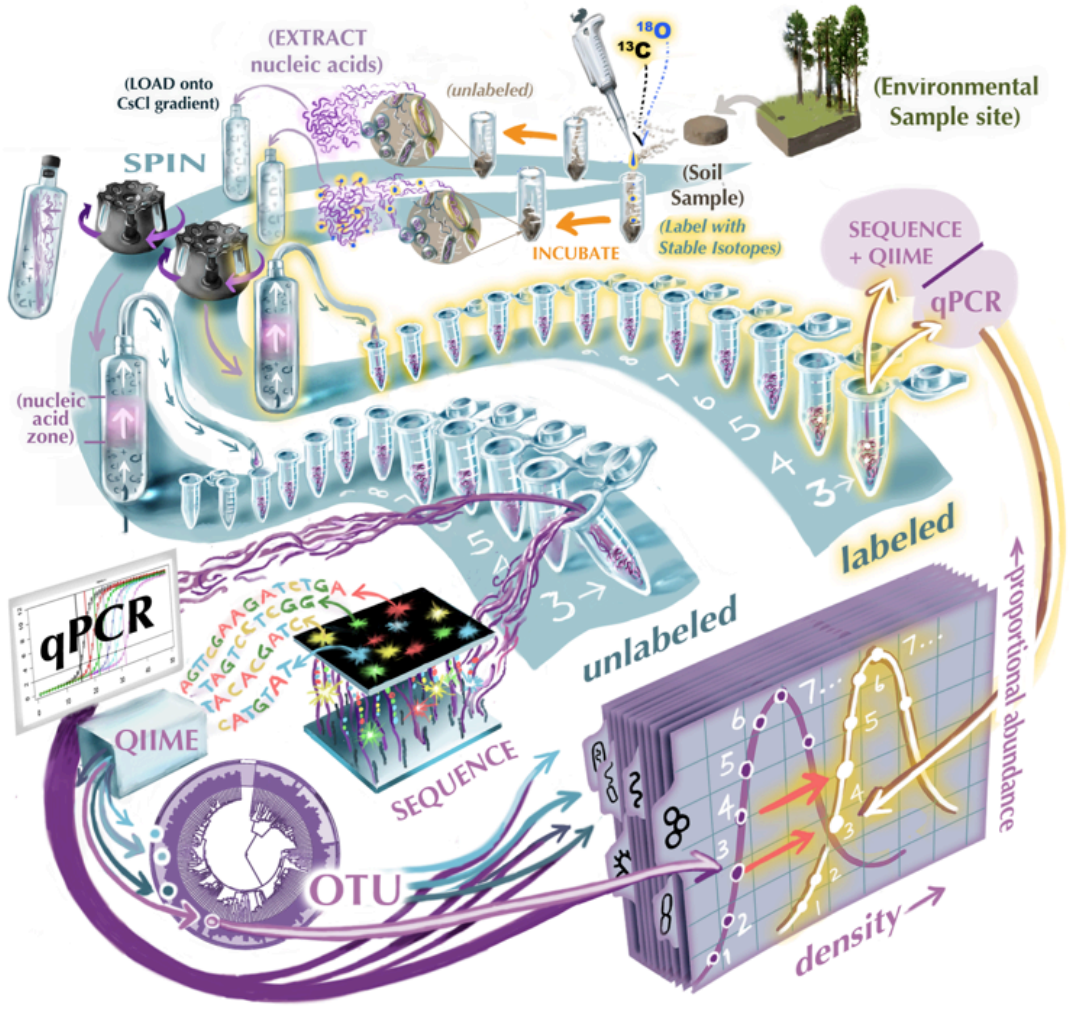

detail in the Appendix below. We used bootstrap resampling (1000 iterations) of replicates within each treatment to estimate 90% confidence intervals for all calculated quantities. Calculations were performed in R (R Core Team 2014).

In pure culture experiments, ^{18}O composition of *E. coli* DNA was strongly related to the ^{18}O composition of water in the growth medium, supporting the notion that oxygen from water is quantitatively incorporated into the DNA of growing organisms ($P<0.001$, $R^2 = 0.976$, Figure 2A). The slope of the relationship, 0.334 ± 0.017 (n=15), indicates the proportion of oxygen in *E. coli* DNA that was assimilated from water. Furthermore, the shift in density of *E. coli* DNA with ^{18}O incorporation matched very well the theoretical prediction of the model of isotope substitution in the DNA molecule (Figure 2B). Thus, ultracentrifugation in cesium chloride can serve as a quantitative mass separation procedure, resolving variation in isotope tracer incorporation into DNA.

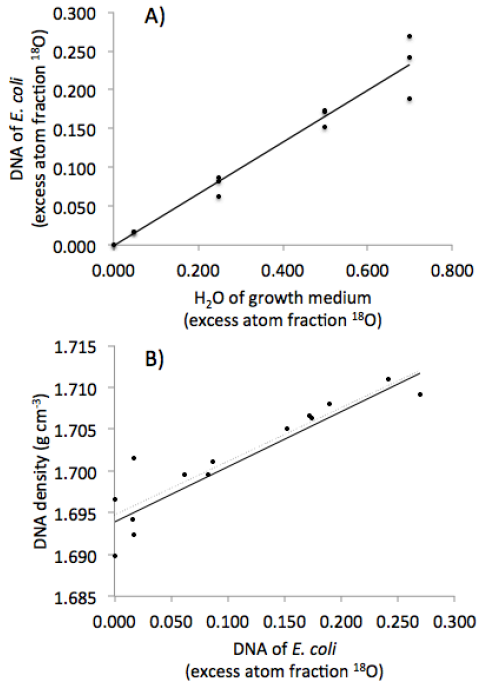

Figure 2. A. The ^{18}O composition of *E. coli* DNA as a function of the ^{18}O composition of water in the growth medium. Solid line is the regression ($^{18}O_{DNA}$ = -0.098 (0.680) + 0.334 (0.017) x $^{18}O_{H_2O}$, n=15, $P<0.001$, $R^2=0.976$). B. Theoretical and observed relationship between the 18O composition and the density of DNA of E. coli. Theoretical relationship is show by the dashed line, whereas the solid line is the regression on the observed data (points).

In soil incubations, the density of DNA increased in response to isotope addition, and the degree of increase varied among taxa and treatments (Figure 3, Figure 4). For example, the weighted average density of a member of the family Micrococcaceae did not change (difference in means: -0.0002 g cm^{-3}, 90% CI -0.0046 to 0.0049 g cm^{-3}) in response to ^{18}O-H_2O in the absence of a supplemental carbon source (Figure 3A), but it increased by 0.0169 g cm^{-3} (90% CI, 0.0146-0.0194 g cm^{-3}) because glucose addition stimulated ^{18}O incorporation (Figure 3B). This bacterial taxon was therefore not growing in unamended soil, but grew (i.e., synthesized new DNA) after glucose addition. The DNA of an unidentified genus in the family Pseudonocardiaceae, also exhibited no change in density in the absence of glucose (0.0005 g cm^{-3}, -0.0033 to 0.0045 g cm^{-3}), and exhibited only a slight but significant increase in response to glucose addition (0.0040 g cm^{-3}, 0.0015 to 0.0070 g cm^{-3}, Figure 3C&D). By contrast, members of the genus *Herpetosiphonales* were synthesizing new DNA in the soil without added glucose (difference in means: 0.0124, 90% CI, 0.0105 to 0.0143 g cm^{-3}) and were unaffected by glucose amendment (difference in means: 0.0110 g cm^{-3}, 90% CI, 0.0088 to 0.0133 g cm^{-3}) (Figure 3E & F).

Changes in the density of DNA among taxa in response to isotope addition translate directly to quantitative variation in isotope composition, expressed here as excess atom fraction ^{18}O (Figure 4 A and B) and ^{13}C (Figure 4 C). The median change in weighted average density required to shift

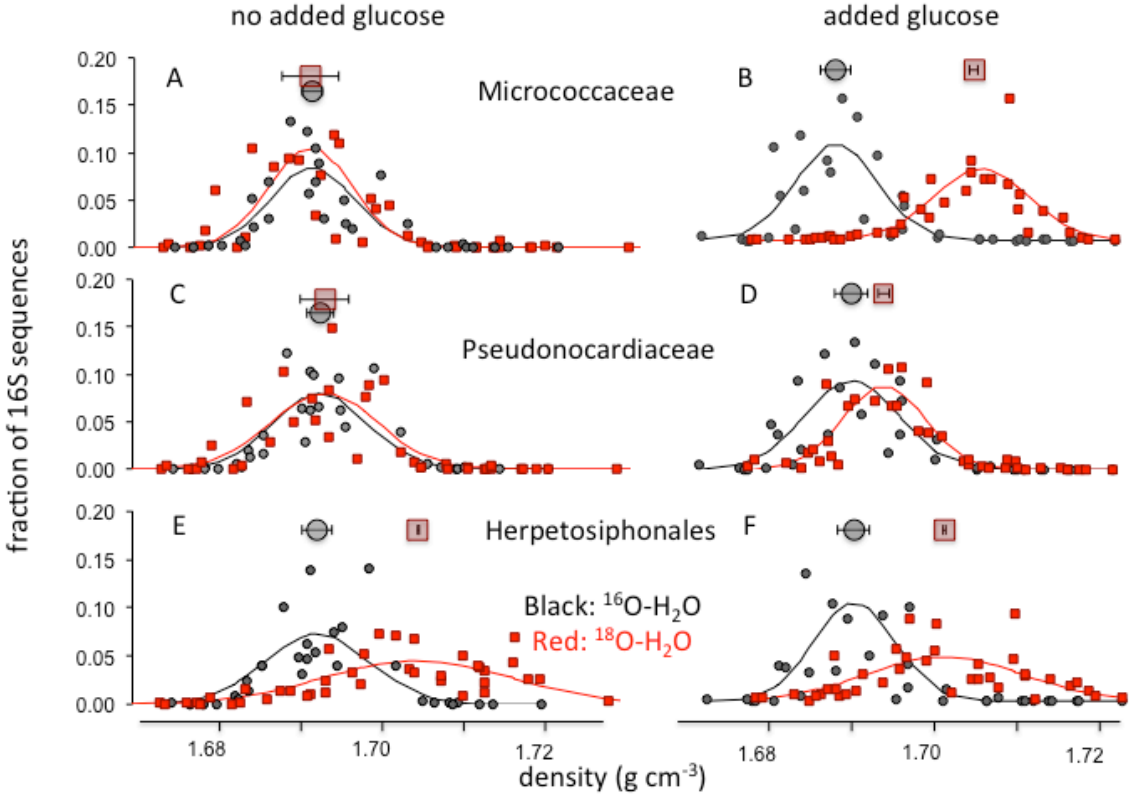

Figure 3. Frequency distribution of the 16S rRNA gene as a function of density of DNA for three different taxa with no added glucose (left side panels) and with added (natural abundance $\delta^{13}C$) glucose (right side panels) for three different taxa: unidentified members of the family Micrococacceae (A & B) and Pseudonocardiaceae (C & D), and genus *Herpetosiphonales* (E & F). Black symbols show the density distribution for the incubation where all substrates had natural abundance isotope composition, and red symbols show the distribution with ^{18}O-labeled H_2O. The distribution of densities for each taxon in each replicate yielded an estimate of the weighted average density for that taxon, the average of which is indicated by the large points black and red points for each taxon and treatment (bars show SEM with n=3).

the bootstrapped 5% confidence limit above zero was 0.0034 g cm^{-3} for ^{18}O, and 0.0042 g cm^{-3} for ^{13}C, corresponding to an increase of 0.051 in atom fraction ^{18}O and of 0.078 for ^{13}C.

More than half of the bacterial taxa did not exhibit any detectable excess ^{18}O enrichment under control conditions without an added carbon substrate (Figure 4A). Of the 60 taxa that did exhibit a detectable increase in the average density of DNA without an added carbon source, the corresponding values of excess atom fraction ^{18}O ranged from 0.061 ± 0.058 in a member of the order, Rhodospirillales, to 0.261 ± 0.023 in a representative of the genus *Arenimonas*. With added glucose, 124 of the 130 taxa exhibited non-zero excess atom fraction ^{18}O, averaging 0.153 ± 0.044 (Figure 4B), with a minimum of 0.061 ± 0.028 in a member of the genus Lysinibacillus and a maximum of 0.327 ± 0.042 in a member of the family Coxiellaceae. Thus, bacterial taxa in this

soil exhibited quantitatively different shifts in excess ^{18}O, indicating different rates of DNA synthesis under control conditions (i.e., added water) and in response to added glucose (Figure 4A and 4B). Excess atom fraction ^{13}C reflects direct utilization of the added glucose (Figure 4C), and ranged from no significant enrichment in a member of the family Procabacteriaceae (-0.059 ± 0.117) to over half of the carbon atoms comprising ^{13}C in the DNA of a member of the Micrococcaceae (0.525 ± 0.034). For 72 taxa, excess atom fraction ^{13}C was greater than zero (90% confidence intervals did not overlap zero) whereas the change in atom fraction ^{13}C for 58 taxa was not distinguishable from zero.

For more details on the mathematics used to convert density to atom fraction isotope incorporation, please see the Appendix to this report.

1) Quantitative Stable Isotope Probing

B. Modeling Microbial Growth As one example of the type of methodological development possible with the new technique developed here, we built a mathematical model to convert density shifts and thus isotope enrichment to estimate vital rates of bacterial populations: i) growth rate, a function of the incorporation of ^{18}O from labeled water into DNA, and ii) mortality rate, a function of the disappearance of gene sequences carrying a natural abundance isotopic signature. Details of this model are provided in the text that follows.

Understanding how population-level dynamics contribute to ecosystem-level processes is a primary focus of ecological research and has led to important breakthroughs in the ecology of macroscopic organisms. However, the inability to measure population-specific rates, such as growth, for microbial taxa within natural assemblages has limited ecologists' understanding of how microbial populations interact to regulate ecosystem processes. Here, we use isotope incorporation within DNA molecules to model taxon-specific population growth in the presence of ^{18}O-labeled water. By applying this model to phylogenetic marker sequencing data collected from stable-isotope probing studies, we estimate rates of growth, mortality, and turnover for individual microbial populations within soil assemblages. When summed across the entire bacterial community, our taxon-specific estimates are within the range of other whole-assemblage measurements of bacterial turnover. Because it can be applied to environmental samples, the approach we present is broadly applicable to measuring population growth, mortality, and associated biogeochemical process rates of microbial taxa for a wide range of ecosystems and can help reveal how individual microbial populations drive biogeochemical fluxes.

In this work, we extend the qSIP approach toward the integration of population- and ecosystem-level processes by calculating taxon-specific population growth and mortality rates (d^{-1}) for all detectable bacterial and archaeal taxa following rewetting of a seasonally dried semiarid grassland soil. By estimating taxon-specific rates of microbial growth and turnover, we highlight the potential for linking population dynamics of microbial taxa to ecosystem-level processes within highly diverse natural or engineered assemblages. For the methods and mathematical model, please see the published paper (Koch et al. 2018, Ecosphere doi.org/10.1002/ecs2.2090)

Our analysis yielded population growth and mortality rates for 326 bacterial and archaeal taxa distinguished at the level of genus, representing at least 22 different phyla. Nearly three-quarters (74%) of all soil taxa became enriched with ^{18}O, as determined by the 90% CIs for excess atom fraction exceeding zero (Fig. 1). The CIs for excess atom fraction ^{18}O overlapped zero for 26% of taxa. No taxon had negative ^{18}O enrichment. This pattern of isotopic enrichment indicates that (1) the qSIP method of quantifying isotopic incorporation was sufficiently robust to avoid falsely detecting a decrease in ^{18}O enrichment and (2) most taxa incorporated ^{18}O atoms into newly synthesized DNA, supporting the conclusion that these taxa produced new cells during the incubation.

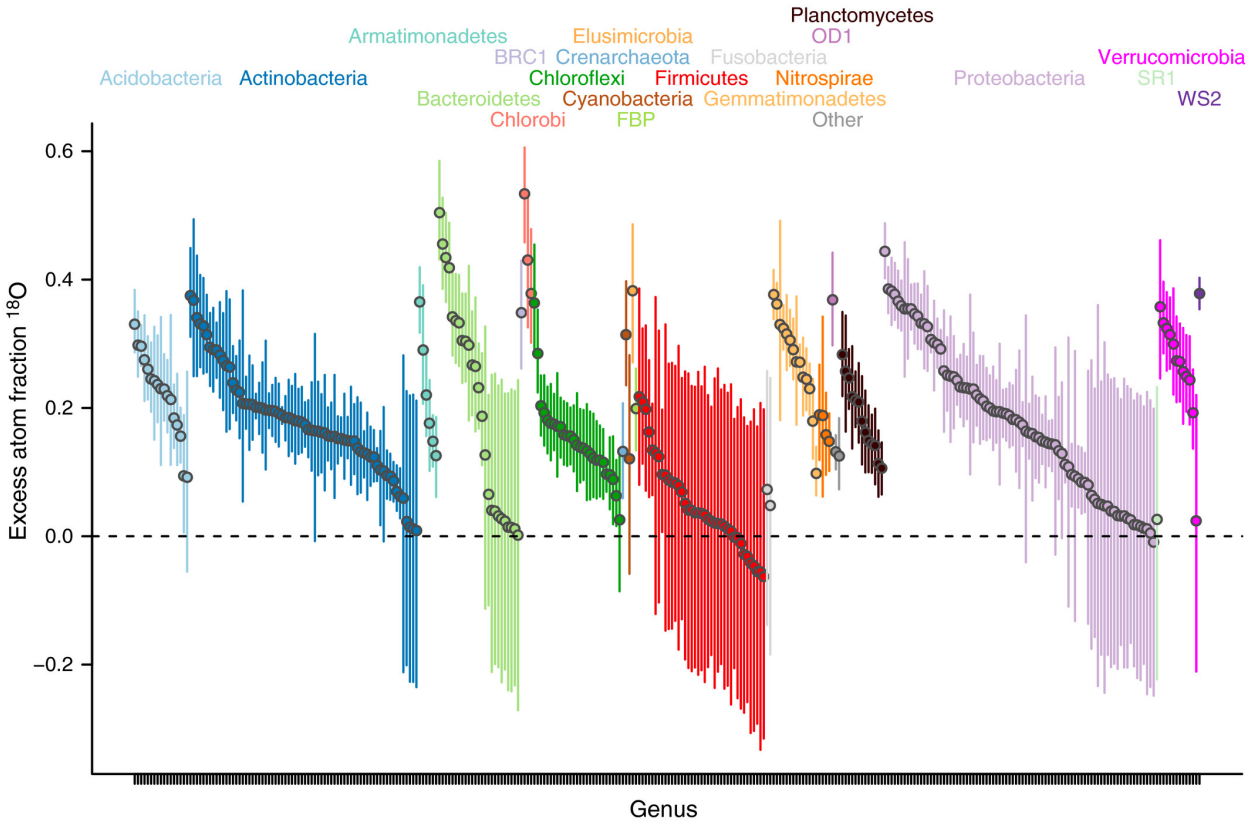

Figure 4. Isotope enrichment in bacterial general after exposure to 18O-labeled water, with 90% confidence limits illustrating the potential power of the qSIP technique.

The ability to estimate taxon-specific population dynamics within microbial assemblages has important implications for ecology. Resolving population growth rates for co-occurring microbes enables more precise inferences of species interactions like competition and predation, the outcomes of which depend strongly on vital rates (Tilman 1977). For example, microbial interaction networks constructed from relative abundance data alone may not accurately reflect species interactions (Berry and Widder 2014). Incorporating additional information on growth, mortality, and turnover rates—estimated via qSIP—could enable detecting the fingerprints of species interactions. Specific interactions among organisms—mutualism, amensalism, competition, and predation—produce specific expectations about vital rates of ostensibly interacting taxa, and in this way, likely interactions can be discerned from spurious correlations.

Because the qSIP approach can inform our understanding of such microbial interactions, it has the potential to vastly extend the size spectrum of organisms included in food web analyses (Schmid-Araya et al. 2002).

Measuring taxon-specific growth and mortality can also facilitate confronting existing community and ecosystem models with highly resolved population data from microbial communities. Such tests would improve our understanding of the role of microbes in ecosystems and advance ecological theory (Prosser et al. 2007). For example, by applying qSIP to derive time series of abundance, growth, and mortality, classical theories of succession (Odum 1960, Connell and Slatyer 1977, Tilman 1985) and community assembly (Post and Pimm 1983, Moyle and Light 1996, Tilman 1999) could be tested for microbial assemblages, something only rarely possible for macroscopic organisms. Furthermore, the ability to link population dynamics of individual microbial taxa to biogeochemical processes might illuminate whether a handful of hyper-abundant foundation taxa (Ellison et al. 2005) drive element fluxes, or whether they are instead regulated by rare keystone taxa (Power et al. 1996). Applications of qSIP in this vein have already revealed that microbial activity varies with phylogeny (Morrissey et al. 2016) and that the enigmatic phenomenon of priming—in which pulses of new organic matter enhance the decomposition of older organic matter—is mediated by taxa across the phylogenetic spectrum (Morrissey et al. 2017).

Estimating microbial population growth also paves the way for making taxon-specific estimates of prokaryotic production. For example, by applying to our data the simplifying assumptions that all prokaryotic taxa contain six 16S rRNA gene copies per cell (despite the known variability; Crosby and Criddle 2003, Acinas et al. 2004, Case et al. 2007) and that an average cell contains 0.1 pg carbon (C; Bölter et al. 2002), then assemblage-level prokaryotic production was 2.76 $\mu g\ C \cdot [g\ soil]^{-1} \cdot d^{-1}$ and assemblage-level loss of C to cell death was 22 times higher. The dominant taxon in terms of production comprised unidentified members of the order RB41 (phylum Acidobacteria), which was extremely abundant but grew at a relatively modest rate. Conversely, members of the order Sphingobacteriales (phylum Bacteroidetes) were not particularly abundant, but had high productivity owing to their rapid growth rates. Future applications of qSIP to estimate taxon-specific production could be improved by accounting for taxonomic variation in the number of 16S rRNA gene copies per cell, which typically range from 2 to 15 (Markowitz et al. 2012, Langille et al. 2013). However, even with that additional information, absolute abundances would still be approximate, due to the challenges of quantitatively extracting DNA from free-living cells (Martin-Laurent et al. 2001), as well as amplification and sequencing biases (Kanagawa 2003, Kozarewa et al. 2009, Tedersoo et al. 2010). The inability to measure absolute abundance and cell size of microbes remains a constraint on our ability to link taxon-specific fluxes to biogeochemical processes. Nevertheless, developing tools for even coarse estimates of taxon-specific production will advance our ability to connect biogeochemical fluxes in ecosystems with their population- and community-level drivers (Hutchinson 1942, Lindeman 1942).

A high level of phylogenetic resolution in population dynamics and element fluxes opens the door to a more intricate understanding of microbial natural history (Lazcano 2011). In the same way that detailed natural history knowledge has informed the ecology of macroscopic organisms (Tewksbury et al. 2014), uncovering the unique responses of different bacteria to environmental conditions can lead to better predictions for how ecosystems respond to environmental change. For example, Blazewicz et al. (2014) found high bacterial and fungal mortality and population turnover following rewetting of a northern California grassland soil.

Despite those changes in dynamics, population abundances remained relatively stable. Although we observed net decreases in population abundances, our data similarly suggest that such high mortality and turnover are shared by most of the bacterial taxa present in rewetted soil. Only one genus, Sporocytophaga (phylum Bacteroidetes), had a net positive rate of reproduction in response to rewetting. Sporocytophaga is adapted to dry conditions and readily forms microcysts in desiccated soils (Grace 1951, Reichenbach 2006). Our observations that this genus also had low mortality and relatively high rates of new growth following soil rewetting suggest that it may be able to take advantage of rapidly increasing soil moisture and the accompanying massive cell death of other taxa. In contrast to Sporocytophaga, we found that all members of the class Clostridia (phylum Firmicutes) had rates of new growth indistinguishable from zero, indicating that this group may respond more slowly to increases in soil moisture, possibly as oxygen becomes depleted.

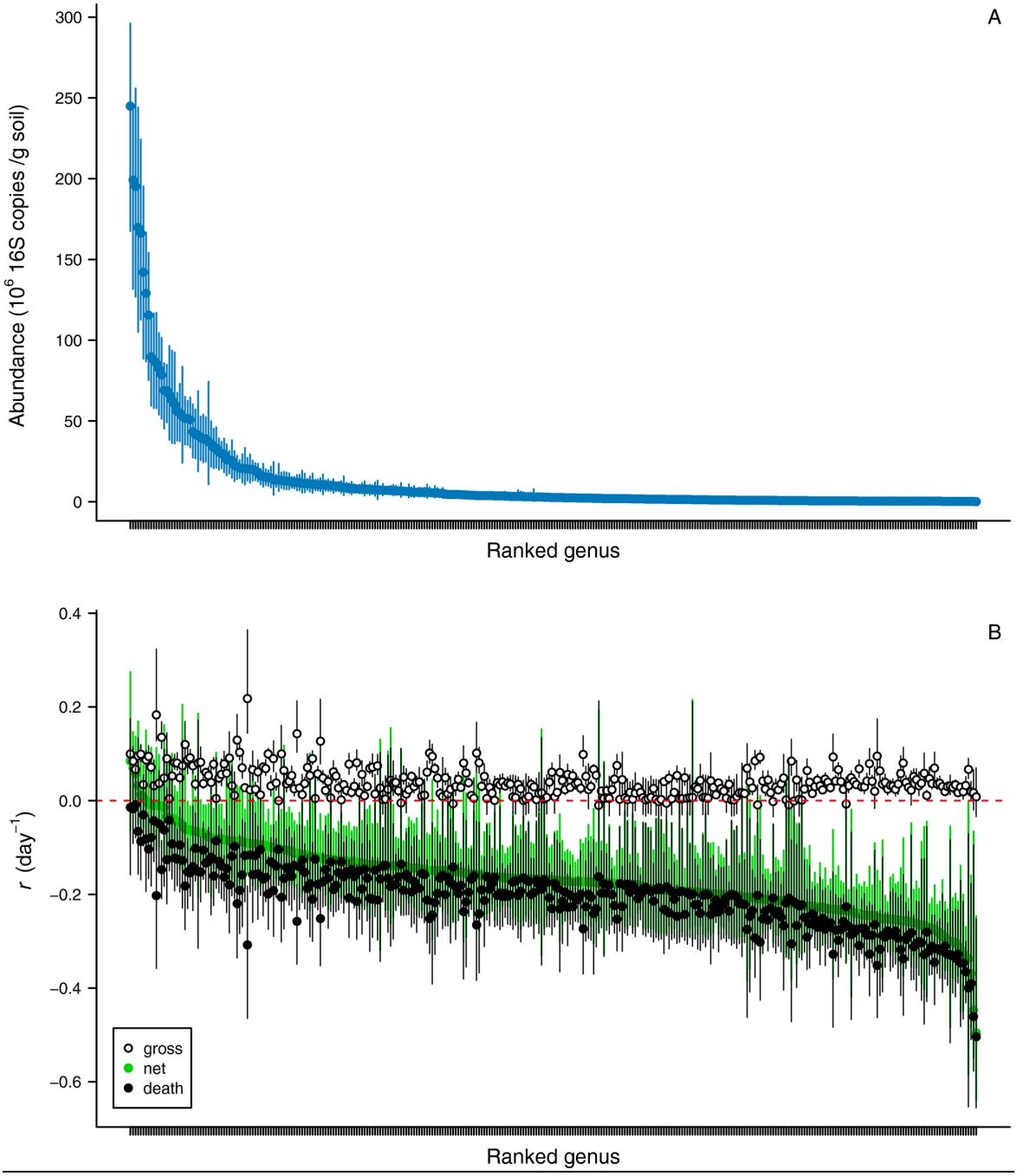

Figure 5. (A) Taxon-specific abundances of 16S rRNA gene copies at the end of the rewetting incubation (day 10) were approximately lognormally distributed, whereas (B) population growth rates (r) followed a normal distribution across genera. Nearly all taxa declined in abundance in response to soil rewetting (net population growth rate, $r < 0$; green circles) because mortality rates (d, filled black circles) outweighed rates of reproduction (b, open circles). Points indicate bootstrapped medians; bars are 90% confidence intervals. Genera are ranked independently in each panel.

2) Priming effect and the bacterial community ecology of organic matter degradation

Our second objective in this project was to use our new method to identify microorganisms oxidizing native soil organic carbon in response to environmental forcings operating on time scales of days to decades. We met this goal in an experiment evaluating the soil priming effect, an experiment in which we applied 13C-labeled glucose to track organisms utilizing the pulse of labile carbon that elicits priming, along with 18O-labeled water that tracks changes in microbial growth rates. Both isotopes were interpreted using the qSIP quantitative framework. The background for this work is the realization that microorganisms perform most decomposition on Earth, mediating carbon (C) loss from ecosystems, and thereby influencing climate. Yet, how variation in the identity and composition of microbial communities influences ecosystem C balance is far from clear. Using quantitative stable isotope probing of DNA, we show how individual bacterial taxa influence soil C cycling following the addition of labile C (glucose). Specifically, we show that increased decomposition of soil C in response to added glucose (positive priming) occurs as a phylogenetically diverse group of taxa, accounting for a large proportion of the bacterial community, shift toward additional soil C use for growth. Our findings suggest that many microbial taxa exhibit C use plasticity, as most taxa altered their use of glucose and soil organic matter depending upon environmental conditions. In contrast, bacteria that exhibit other responses to glucose (reduced growth or reliance on glucose for additional growth) clustered strongly by phylogeny. These results suggest that positive priming is likely the prototypical response of bacteria to sustained labile C addition, consistent with the widespread occurrence of the positive priming effect in nature.

The priming effect is often postulated to involve two distinct bacterial groups: one responds to the labile substrate by utilizing it as a carbon source to grow faster ("r-strategists"), and the other, through some signaling pathway or change in the resource environment, increases its growth by utilizing native soil organic matter ("K-strategists"). If this dichotomous sorting of resource strategy occurs consistently to explain the priming effect, then we expect to observe the relationship shown in Figure 6. **First**, the r-strategists will increase their growth rate when utilizing glucose to grow, with a slope of approximately 2 between the change in at% excess 18O (x axis) and at% excess 13C (y axis). This relationship reflects the fact that around 50% of the oxygen in newly synthesized DNA comes from water (the other half from organic matter). Second, once priming begins to occur, a new group of organisms will become apparent, organisms that exhibit no enrichment in the originally applied 13C, but with an increase in 18O composition reflecting their increased growth rate. In this way, we can qualitatively and quantitatively distinguish between these postulated resource strategies and how they contribute to the soil priming effect.

Some of the results from our experiment supported this conceptual model, in that organisms that grew using the added glucose, as seen by their increase in 13C content, also increased their 18O content, with a slope of around 2 for the 13C to 18O relationship. This is what we observed when no priming was seen (Figure 7).

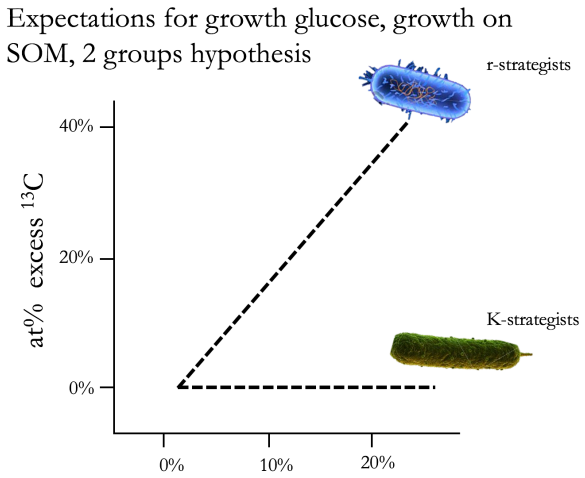

Figure 6

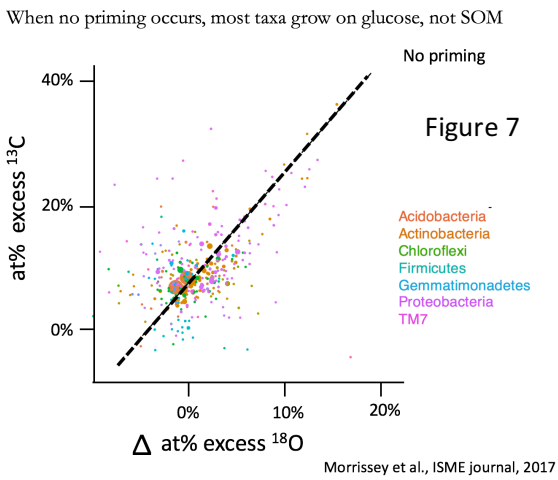

Figure 7

However, later in the experiment, soils did exhibit priming: increased oxidation of native soil organic matter in response to the pulses of glucose availability. And when this happened, we saw a strikingly different pattern that deviated from the 2-groups model (Figure 8).

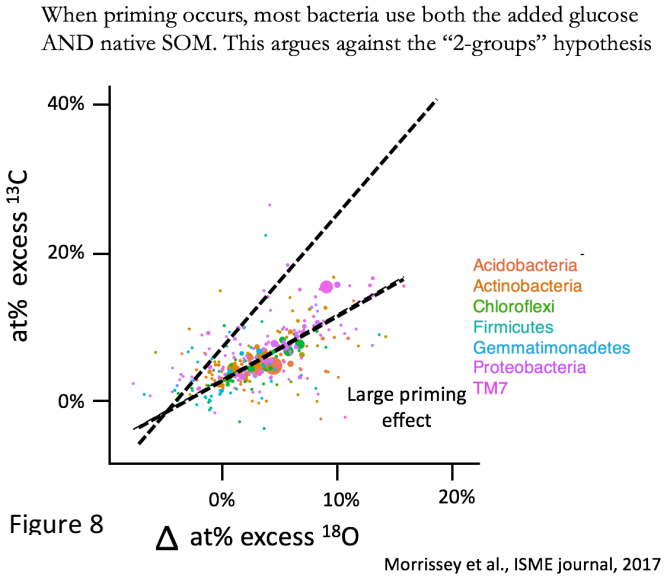

Figure 8

In the soil we assessed, positive priming was caused by the majority of soil bacteria, organisms that were not phylogenetically constrained, suggesting that the priming effect may not depend upon specialized phylogenetic groups. Our findings also suggest that many bacterial taxa can exhibit plasticity with regard to C use, changes in C use that could underlie the emergence of positive priming following the addition of labile C. Examining these dynamics in a broad range of soils could test whether this ubiquity of priming across bacteria biodiversity contributes to the widespread occurrence of positive priming in soil.

3) The third objective of this project was to use taxon-specific profiles of microorganisms to test the hypothesis that there is a phylogentic imprint on the soil carbon cycle. We tested this idea in several contexts, including the priming effect (described above), and published this in two papers in the ISME journal, one of the premier journals for microbial ecology.

This work begins from the notion that phylogeny is an ecologically meaningful way to classify plants and animals, as closely related taxa frequently have similar ecological characteristics, functional traits and effects on ecosystem processes. For bacteria, however, phylogeny has been argued to be an unreliable indicator of an organism's ecology owing to evolutionary processes more common to microbes such as gene loss and lateral gene transfer, as well as convergent evolution. Here we use advanced stable isotope probing with ^{13}C and ^{18}O to show that evolutionary history has ecological significance for in situ bacterial activity. Phylogenetic organization in the activity of bacteria sets the stage for characterizing the functional attributes of bacterial taxonomic groups. Connecting identity with function in this way will allow scientists to begin building a mechanistic understanding of how bacterial community composition regulates critical ecosystem functions.

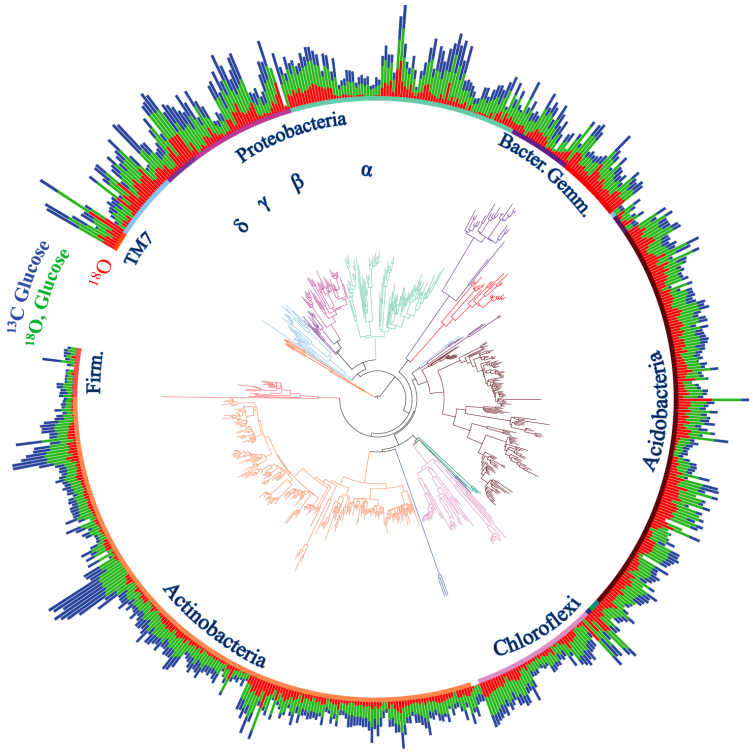

Figure 1 Phylogenetic tree (based on 16S rRNA gene sequences) and isotope incorporation of bacterial taxa in soil. Bars are proportional to the excess atom fraction of ^{18}O or ^{13}C of each taxon's DNA after incubation with ^{13}C-glucose (blue) or $H_2^{18}O$ in the presence (green) or absence (red) of natural abundance glucose. Tree is colored by the phylogenetic group.

4) Multi-Isotope Detection in Microbial Samples

Bulk RNA and DNA

We have developed a new method to rapidly and simultaneously analyze isotopic enrichment of bulk RNA and DNA for multiple elements (^{13}C, ^{15}N, ^{18}O) using NanoSIMS. This is a powerful approach to use with stable isotope probing (SIP) experiments, where it is ideal to gain an understanding of microbial activity and obtain an average isotopic enrichment for community nucleic acids (and thus confirm enrichment) prior to SIP processing. However, the standard approach for analyzing isotopic enrichment in nucleic acids uses Isotope Ratio Mass Spectrometry (IRMS) and requires microgram quantities of generally limited and precious sample. Even when sufficient amounts of RNA or DNA are available, IRMS can only analyze a single isotope at a time. Our newly developed approach uses only small quantities (~100 ng) of valuable samples while allowing us to analyze multiple isotopes simultaneously. Our approach utilizes the following steps: 1) UV cross link bulk RNA or DNA to indium tin oxide coated glass slides (Fig 5), 2) Wash the slide to remove impurities 3) Detect isotopic enrichment of RNA or DNA using NanoSIMS (Fig 5).

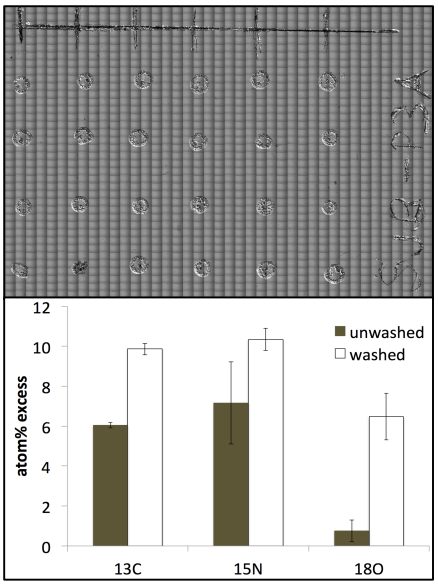

Fig 5. Top: ITO-coated glass slide with RNA spots for NanoSIMS prior to washing the slide. Bottom: Simultaneous isotopic measurements for 50 ng of a single RNA sample with two different sample preparation conditions.

To test if this approach is quantitative, we produced standard curves of bulk RNA and DNA enrichment using RNA and DNA from pure cultures incubated in defined media with a range of isotopic enrichment for ^{13}C and ^{15}N. We then analyzed the bulk RNA and DNA standards at several sample concentrations (0.5, 5, 50, and 100 ng DNA or RNA) and isotopic concentrations (0, 1, 10, 20, 40, 60, 80, 100 at% ^{13}C and ^{15}N) via NanoSIMS. The 100 ng DNA samples produced ideal linear standard curves for the entire range of isotope enrichment (Fig 6), whereas the lower concentration samples appeared to be below detection limits for our current approach (data not shown). The 100 ng bulk RNA samples also produced linear standard curves between 0-40 at% ^{13}C and ^{15}N. These results indicate that this approach is quantitative, and it should be highly valuable for many general stable isotope tracing approaches.

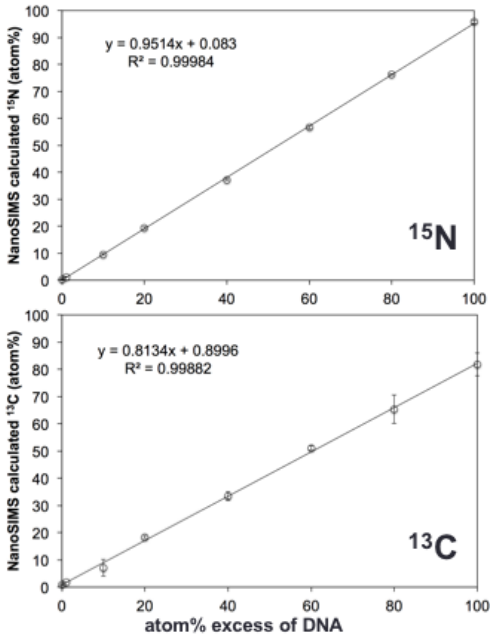

Fig 6. NanoSIMS Bulk DNA analysis of 13C and 15N enriched pure culture standards.

In a proof of concept experiment, we incubated mixed conifer soil from Flagstaff, AZ with different treatments of N and C to quantify how N assimilation into microbial RNA changed with N species and C addition. Our treatments

were: 1) $^{15}NH_4$, 2) ^{13}C-glucose and $^{15}NH_4$, 3) $^{15}NO_3$, and 4) ^{13}C glucose and $^{15}NO_3$. We found no evidence of ^{15}N enrichment in bulk RNA from NO_3 or NH_4 treatments, but significant enrichment in ^{15}N and ^{13}C in the N plus glucose treatments (Fig 7). Results indicate that this approach can be used to track and quantify the assimilation of labeled substrate into complex mixed microbial communities.

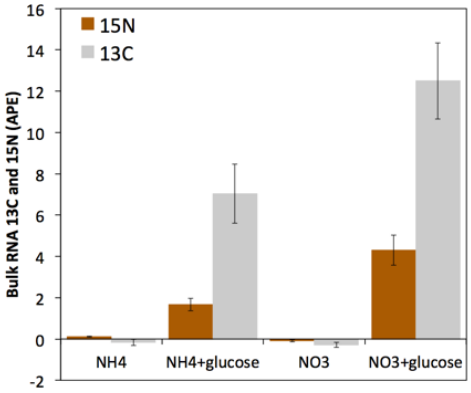

Fig 7. Mixed community bulk RNA isotopic composition from soil incubations

Whole Cells

Pure culture cells were incubated with substrate enriched with different levels of ^{13}C, ^{15}N, and ^{18}O. Whole cells were then NanoSIMS analyzed for ^{13}C, ^{15}N, and ^{18}O (Table 1). These results indicate that it is possible to quantitatively measure three isotope species of interest simultaneously in the same sample. This multiple element isotope analysis can be broadly applied to differentiate whole community activity ($H_2{}^{18}O$) from substrate-specific activity (with ^{13}C or ^{15}N substrates) an could be combined with a range of environmental microbiological approaches such as single cell genomics, SIP targeted fluorescence in situ hybridization, and organism-organism interaction studies.

Table 1. Isotopic values for incubation substrate and measured isotopic values for whole cells of *Bacillus cereus* using NanoSIMS. (Note: "known at% ^{15}N substrate" determined by mixing commercially available ^{15}N-enriched compounds with natural abundance compounds. All other values measured using Nano-SIMS).

Treatment	Known at% ^{15}N Substrate	Measured at% ^{15}N of Cell	Known at% ^{13}C Substrate	Measured at% ^{13}C of Cell	Known at% ^{18}O Substrate	Measured at% ^{18}O of Cell
High	99	54.5	99	68.3	95	35.0
Medium	50	24.7	50	34.0	50	11.2
Low	0.37	0.33	1	1.0	0.2	0.20
Control	0.37	0.37	1	1.0	0.2	0.19

Chip-SIP

We have confirmed that Chip-SIP can detect ^{18}O in addition to ^{13}C and ^{15}N (Fig. 8). $H_2{}^{18}O$ is an ideal substrate to identify active populations, as all known organisms use water, and this is the first evidence that ^{18}O can be quantified simultaneously with ^{13}C and ^{15}N using the Chip-SIP approach. $H_2{}^{18}O$ in conjunction with ^{13}C and ^{15}N identifies all community members that are active in addition to the subsets of community members that are consuming either the C or N substrate of interest. Newly developed ^{18}O Chip-SIP will offer a powerful view into the population dynamics of the active organisms in complex microbial communities.

A primary set of Chip-SIP probes was designed for our experimental soils using our automated probe-design pipeline (described below) and RNA sequence data from these soils. These probes were printed on a microarray, and fluorescently labeled RNA was hybridized to the array (Fig. 9). Fluorescence data from several soil experiments were used as a final filter to down-select probes in order to create an optimized probe-set for our soils. This optimized probe set has been printed on new arrays that were applied to determine relative C and N consumption for different microbial taxa using RNA from the N assimilation experiment described above in the Bulk RNA and DNA section (Fig 10).

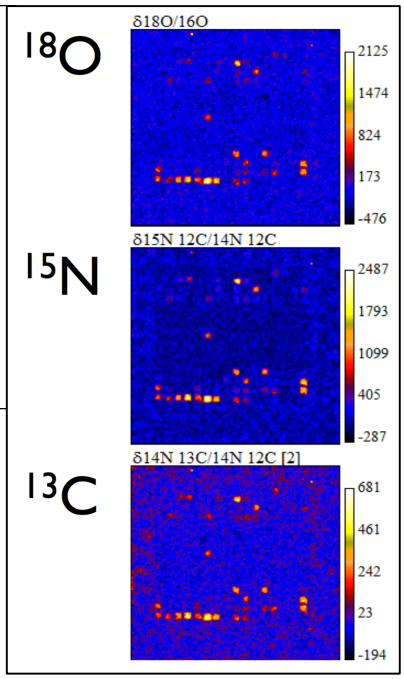

Fig. 8: Simultaneous NanoSIMS imaging of ^{18}O, ^{15}N, and ^{13}C labeled RNA hybridized to a Chip-SIP phylogenetic microarray. *Bacillus* RNA was enriched to the following atom percent values: 58% ^{15}N, 68% ^{13}C, 35% ^{18}O). The detection limit for ^{13}C and ^{15}N is 0.5% and 0.1%, respectively.

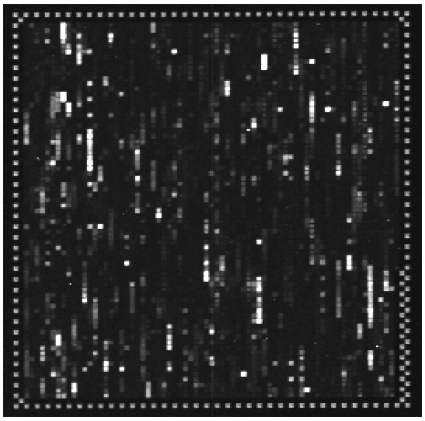

Fig. 9: Fluorescence scan of microarray with our full probe-set targeting our experimental soil communities.

In summary, hybridized chips were analyzed via NanoSIMS to quantify isotopic enrichment for specific taxonomic probe sets. Enrichment values were corrected for relative taxon abundance using fluorescence microarray data to calculate hybridization correction enrichment (HCE) which represents relative consumption. Results clearly show differential substrate consumption patterns for different taxa. For example, Actinobacteria dominated C consumption when NO_3^- was added, but not when NH_4^+ was added (Fig 10 and 11).

	NH_4 + Glucose		NO_3 + Glucose		
	^{13}C	^{15}N	^{13}C	^{15}N	
Acidobacteria	0.14	0	0.06	0.08	
Actinobacteria	0.12	0	0.46	0.1	
Bacteria_k	0.16	0.43	0.13	0.14	
Bacteroidetes	0.07	0	0.04	0.32	
Chloroflexi	0.05	0	0	0	
Proteobacteria	0.46	0.57	0.31	0.35	

Fig 10. Relative C and N consumption at the phylum level. Numbers represent normalized HCE (hybridization corrected values) with larger numbers indicating higher relative consumption for a given isotope within a single treatment.

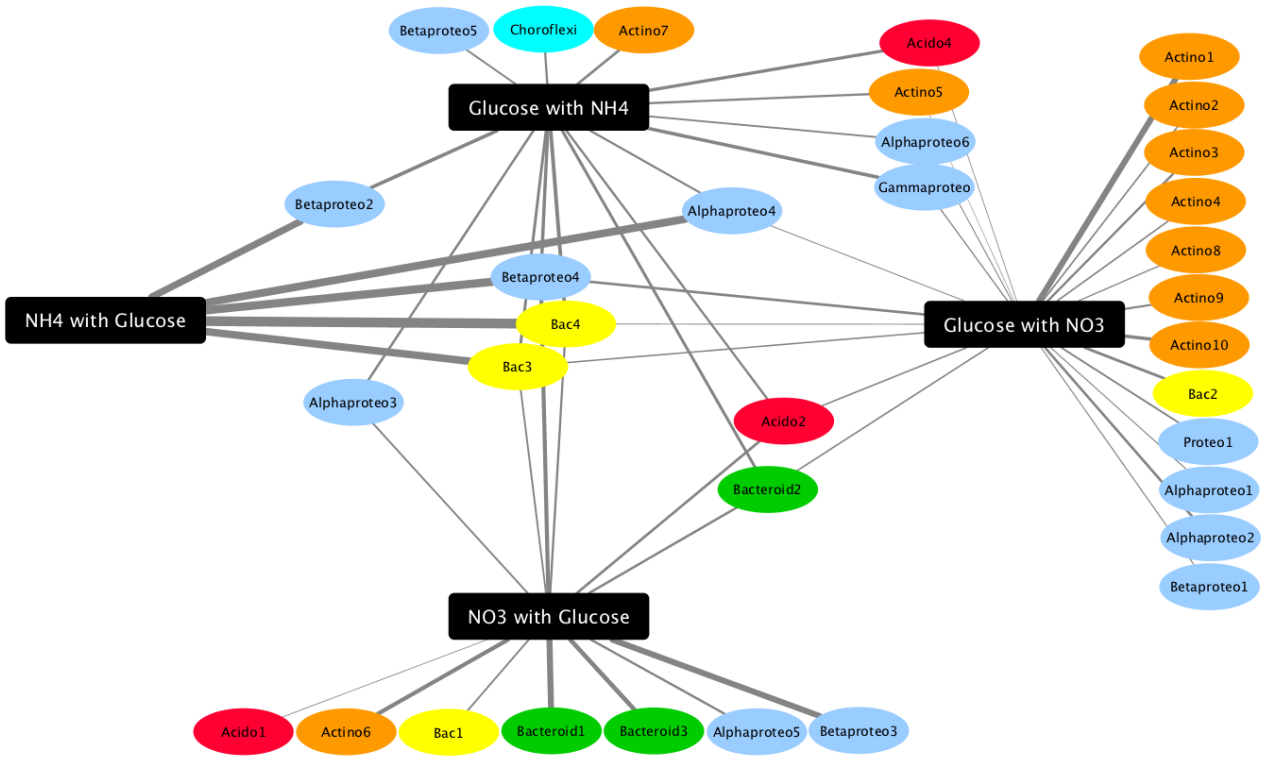

Fig 11. Network showing uptake patterns of four substrates by different bacterial taxa in Arizona soil determined via Chip-SIP. The thicknesses of the lines are proportional to the substrate incorporation rates based on HCE calculations. 'Glucose with NH4' is glucose consumption with added NH_4^+. 'NH4 with glucose' is NH4 consumption with added glucose. Glucose with NO3 is glucose consumption with added NO3. NO3 with glucose is NO3 consumption with added glucose. (Acido=Acidobacteria; Actino=Actinobacteria; Bac=Bacteria kingdom; Bacteroid=Bacteroidetes; Alphaproteo=Alpha-Proteobacteria; Betaproteo=Beta-Proteobacteria; Gammaproteo=Gamma-Proteobacteria)

Chip-SIP Automated Probe Design

We have developed an automated probe design pipeline to accelerate the design of quality custom Chip-SIP arrays from next-generation sequencing datasets, which will facilitate the application of Chip-SIP by the greater scientific community. This pipeline includes a probe specificity check to reduce cross-hybridization between probes. The pipeline accepts a next-generation sequencing dataset (Illumina, 454) and automatically creates operational taxonomic units (OTUs) that include the nearest full-length sequences in the database. This process uses a combination of tree-based and sequence-similarity based OTU-picking. Next, 50 probes are selected for each OTU, and the probes checked for quality. Probes with high GC content, homopolymer runs, and high probability of hairpin formation are removed from the probe set. The remaining probes are then validated *in-silico* by checking the probes against the original database, and two metrics of specificity are computed: the taxonomic specificity, as well as a probe specificity index (PSI). The PSI is calculated by comparing the BLAST % similarity of a full-length sequence representative against each positive hit. This process accounts for redundant internal 17mers, which can make probes less specific. Finally, the probes are ranked based on PSI, which is used to select the top 15 probes

for each OTU. This pipeline will significantly increase our ability to rapidly design accurate probe-sets for different environmental samples and could be broadly applicable to any rRNA microarray probe design.

Products Delivered:

Hungate BA, *Mau RL*, Schwartz E, Caporaso JG, Dijkstra P, van Gestel N, Koch BJ, Liu CM, McHugh TA, Marks JC, Morrissey E, Price LB, 2015. Quantitative Microbial Ecology Through Stable Isotope Probing. *Applied and Environmental Microbiology* 10.1128/AEM.02280-15

Morrissey EM, *Mau RL*, Schwartz E, Caporaso JG, Dijkstra P, van Gestel N, Koch BJ, Liu, CM, Hayer M, McHugh TA, Marks JC, Price LB, Hungate BA, 2016. Phylogenetic Organization of Bacterial Activity. *ISME Journal*. doi: 10.1038/ismej.2016.28

Schwartz E, Hayer M, Hungate BA, Koch BJ, McHugh TA, Mercurio W, Morrissey EM, Soldanova K, 2016. Stable isotope probing with ^{18}O-water to investigate microbial growth and death in environmental samples. *Current Opinion in Biotechnology* 41, 14-18

Hayer M, Schwartz E, Marks JC, Koch BJ, Morrissey EM, Schuettenberg AA, Hungate BA, 2016. Identification of growing bacteria during litter decomposition in freshwater through $H_2{}^{18}O$ quantitative stable isotope probing. *Environmental Microbiology Reports*, doi:10.1111/1758-2229.12475

Morrissey EM, Mau RL, Schwartz E, McHugh TA, Dijkstra P, Koch BJ, Marks JC, Hungate BA, 2017. Bacterial carbon use plasticity, phylogenetic diversity and the priming of soil organic matter *ISME* 11:1890-1899, doi:10.1038/ismej.2017.43

Mau RL, Dijkstra P, Schwartz E, Koch BJ, Hungate BA, 2018. Warming induced changes in soil carbon and nitrogen influence priming responses in four ecosystems. *Applied Soil Ecology* DOI:10.1016/j.apsoil.2017.10.034

Morrissey EM, Mau RL, Schwartz E, Koch BJ, Hayer M, Hungate BA, 2018. Taxonomic patterns in the nitrogen assimilation of soil prokaryotes. *Environmental Microbiology*. 10.1111/1462-2920.14051

Papp, K, Hungate BA, Schwartz E, 2018. Comparison of Microbial Ribosomal RNA Synthesis and Growth through Quantitative Stable Isotope Probing with H218O. Applied and Environmental Microbiology, DOI: 10.1128/AEM.02441-17

Papp K, Mau R, Hayer M, Koch B, Hungate BA, Schwartz E, 2018. Quantitative Stable Isotope Probing with $H_2{}^{18}O$ reveals that most bacterial taxa in soil synthesize new ribosomal RNA. ISME Journal, in press

---

Appendix: Modeling Details

Definitions of indices, parameters, variables, and calculated quantities used in the modeling of bacterial growth rate.

Indices:

i	taxon
j	tube (or 'rep' within a treatment)
k	fraction (within a tube)
t	treatment
c	comparison (pairwise comparison of treatments)
I	number of taxa
J	number of tubes (within a treatment)
K	number of fractions (within a tube)
T	number of treatments
C	number of comparisons

Parameters:

U	proportion of oxygen atoms in DNA that are from environmental water (unitless)
P	number of 16S copies per cell (copies cell^{-1})
L	mass of carbon per cell (pg C cell^{-1})
H_{OXYGEN}	average number of oxygen atoms per DNA nucleotide (constant for all taxa)

Variables:

v	volume of a fraction (same for all fractions and tubes) (µL)
d_t	length of incubation for treatment t (days)
a_{tj}	mass of DNA per mass of soil for tube j of treatment t (µg DNA g soil^{-1})
b_{tj}	mass of DNA added to tube j of treatment t (µg DNA tube^{-1})
f_{tjk}	total number of 16S copies per µL (all taxa combined) in fraction k of tube j of treatment t (copies µL^{-1})
p_{itjk}	proportion of the total number of 16S copies per µL that are taxon i in fraction k of tube j of treatment t (unitless)
x_{tjk}	density of fraction k of tube j of treatment t (g mL^{-1})

Calculated quantities:

y_{itjk}	number of 16S copies per µL of taxon i in fraction k of tube j of treatment t (copies µL^{-1})
y_{itj}	total number of 16S copies per µL of taxon i in tube j of treatment t (copies µL^{-1})
S_{tj}	mass of soil for tube j of treatment t (g soil tube^{-1})
W_{itj}	observed weighted-average density for taxon i in tube j of treatment t (g mL^{-1})
W_{it}	observed weighted-average density for taxon i in treatment t (mean across all tubes in treatment t) (g mL^{-1})
W_i	observed weighted-average density for taxon i assuming no labeling by heavy isotopes (mean across all tubes in all treatments without heavy isotopes) (g mL^{-1})
G_i	guanine + cytosine content of taxon i (unitless)
$H_{CARBONi}$	average number of carbon atoms per DNA nucleotide for taxon i

M_i molecular weight of taxon *i* (technically the molecular weight of the DNA fragment containing the 16S RNA gene for taxon *i*) (g mol^{-1})

$M_{LIGHTic}$ theoretical molecular weight of taxon *i* assuming no labeling by the heavy isotope in comparison *c* (g mol^{-1})

$M_{HEAVYic}$ theoretical molecular weight of taxon *i* assuming some specified level of labeling by the heavy isotope in comparison *c* (g mol^{-1})

$M_{HEAVYMAXic}$ theoretical molecular weight of taxon *i* assuming maximum labeling by the heavy isotope in comparison *c* (g mol^{-1})

M_{REFic} observed molecular weight of taxon *i* in the 'reference' treatment of comparison *c* (g mol^{-1})

M_{LABic} observed molecular weight of taxon *i* in the 'labeled' treatment of comparison *c* (g mol^{-1})

Q_{ic} number of gene copies of taxon *i* in the 'reference' treatment of comparison *c*

$Q_{LIGHTic}$ number of 'light', or unlabeled, gene copies of taxon *i* in the 'labeled' treatment of comparison *c*

$Q_{HEAVYic}$ number of 'heavy', or labeled, gene copies of taxon *i* in the 'labeled' treatment of comparison *c*

Z_{ic} difference in observed weighted-average densities of taxon *i* for the two treatments in comparison *c* (g mL^{-1})

A_{ic} excess atom fraction of the heavy isotope in the 'labeled' vs. 'reference' treatment for taxon *i* for comparison *c* (equivalent to 'atom percent excess' but not expressed as a percent) (unitless)

g_{ic} net *per capita* rate of increase of taxon *i* based on comparison *c* (day^{-1})

F_{ic} flux of carbon into biomass due to taxon *i* based on comparison *c* (pg C g $soil^{-1}$ day^{-1})

Calculating weighted-average density by taxon

For each taxon (*i*), we calculated the number of 16S rRNA gene copies per µL for each fraction (*k*) of each replicate tube (*j*) in each treatment (*t*),

$$y_{itjk} = p_{itjk} \cdot f_{tjk} \tag{1}$$

and summed across all fractions to calculate the total number of 16S rRNA gene copies per µL for each taxon in each replicate tube:

$$y_{itj} = \sum_{k=1}^{K} y_{itjk} \tag{2}$$

We calculated weighted-average densities for each taxon (*i*) in each replicate tube (*j*) for each treatment (*t*) based on the relative number of 16S rRNA gene copies in each density fraction (*k*) as:

$$W_{itj} = \sum_{k=1}^{K} x_{tjk} \cdot \left(\frac{y_{itjk}}{y_{itj}} \right) \tag{3}$$

and calculated the mean across replicate tubes to estimate the taxon-specific weighted average density for each treatment (t):

$$W_{it} = \frac{\sum_{j=1}^{J} W_{itj}}{J} \tag{4}$$

For a given taxon, we calculated the difference in weighted average density between a heavy (^{18}O or ^{13}C) and light (natural abundance) labeling treatment by subtracting the light (W_{i1}) from the heavy (W_{i2}) treatment:

$$Z_{ic} = W_{i2} - W_{i1} \tag{5}$$

Estimating excess atom fraction ^{18}O and ^{13}C

We estimated the excess atom fraction (of ^{18}O or ^{13}C) of each taxon's DNA for the labeled treatment relative to the corresponding unlabeled treatment by modeling the increase in the molecular weight of DNA in the labeled treatment relative to theoretical estimates of unlabeled and fully labeled DNA.

Because there were multiple treatments without heavy isotopes, we included data from all replicate tubes in those unlabeled treatments (e.g. unlabeled treatments with and without added carbon and at different time intervals) to estimate the 'reference' weighted-average density for a given taxon (i):

$$W_i = \frac{\sum_{j=1}^{J} W_{i1j} + \sum_{j=1}^{J} W_{i3j}}{2J} \tag{6}$$

Here, to illustrate our calculations, $t = 1$ and $t = 3$ represent the two experimental treatments with no heavy isotopes. We used the reference weighted-average density for each taxon to estimate taxon-specific guanine + cytosine content using the relationship derived from the pure-culture incubations (described above):

$$G_i = \frac{1}{0.083506} \cdot \left(W_i - 1.646057 \right) \tag{7}$$

Based on the atomic composition of the four DNA nucleotides, the molecular weight of DNA varies with guanine + cytosine content according to:

$$M_i = 0.496 G_i + 307.691 \tag{8}$$

where M_i is the molecular weight of DNA for taxon i with guanine + cytosine content G_i.

Similarly, the average number of carbon atoms per DNA nucleotide also varies with guanine + cytosine content,

$$H_{CARBONi} = -0.5G_i + 10 \tag{9}$$

and can be used to estimate the theoretical maximum molecular weight of newly synthesized DNA for taxon i in the ^{13}C treatment, assuming that 100% of carbon atoms in new DNA are derived from the ^{13}C-labeled substrate:

$$M_{HEAVYMAXic} = M_{LIGHTic} + H_{CARBONi} \tag{10}$$

When replaced by ^{13}C, each carbon atom in a DNA nucleotide accounts for an increase of 1 g mol^{-1} (the weight of one additional neutron) over the molecular weight of DNA for taxon i in the corresponding natural abundance C treatment for comparison c. If no other heavy isotopes are involved in treatment comparison c, then $M_{LIGHTic} = M_i$.

The average number of oxygen atoms per DNA nucleotide is constant ($H_{OXYGEN} = 6$) regardless of guanine + cytosine content, thus

$$M_{HEAVYMAXic} = 2H_{OXYGEN} + M_{LIGHTic} \tag{11}$$

when comparing ^{18}O and natural abundance O treatments because each ^{18}O atom replacing a ^{16}O atom adds 2 g mol^{-1} (the mass of two additional neutrons) to the molecular weight of DNA for taxon i (assuming 100% of oxygen atoms are replaced by ^{18}O atoms in newly synthesized DNA).

We used the measured increase in weighted-average density to estimate the observed average molecular weight of DNA for taxon i in the labeled treatment (i.e., the treatment with ^{18}O or ^{13}C) as:

$$M_{LABic} = \left(\frac{Z_{ic}}{W_{i1}} + 1 \right) \cdot M_{REFic} \tag{12}$$

where $t = 1$ is the corresponding treatment with no heavy isotope and M_{REFic} is the observed molecular weight of taxon i in the treatment with no heavy isotope. If no other heavy isotopes are involved in treatment comparison c, then $M_{REFic} = M_{LIGHTic} = M_i$.

The excess atom fraction of ^{18}O for taxon i was calculated as:

$$A_{ic} = \frac{M_{LABic} - M_{LIGHTic}}{M_{HEAVYMAXic} - M_{LIGHTic}} \cdot 0.99799957 \tag{13}$$

where the constant on the right represents (1 – the proportion of all oxygen atoms that are ^{18}O in VSMOW) (IAEA 1995).

Similarly, the excess atom fraction of ^{13}C for taxon *i* was calculated as:

$$A_{ic} = \frac{M_{LABic} - M_{LIGHTic}}{M_{HEAVYMAXic} - M_{LIGHTic}} \cdot 0.98888767 \quad (14)$$

where the constant on the right represents (1 – the proportion of all carbon atoms that are ^{13}C in VPBD) (IAEA 1995).

Modeling net, per capita rate of increase

We used the increase in densities for taxa in the ^{18}O treatment relative to their densities in the ^{16}O treatment to infer each taxon's intrinsic rate of increase (*g*), and performed analogous calculations for the ^{13}C and ^{12}C additions of the added glucose treatments. We assumed an exponential model of population growth and further assumed that no turnover occurred during either of the 7-day incubation periods.

First, the observed molecular weight of DNA for taxon *i* in the labeled treatment (i.e., the treatment with ^{18}O or ^{13}C) can be expressed as the weighted average of the molecular weights of unlabeled (i.e., pre-existing) and labeled (i.e., newly synthesized) DNA molecules at the end of the incubation period:

$$M_{LABic} = \frac{M_{LIGHTic}Q_{LIGHTic} + M_{HEAVYic}Q_{HEAVYic}}{Q_{LIGHTic} + Q_{HEAVYic}} \quad (15)$$

The quantity $M_{HEAVYic}$ represents the theoretical molecular weight of newly synthesized DNA for taxon *i* in the labeled treatment of comparison *c*, assuming a certain degree of incorporation of the heavy isotope. For the ^{13}C treatment, we assumed that 100% of carbon atoms in newly synthesized DNA were replaced by ^{13}C atoms, and therefore:

$$M_{HEAVYic} = M_{HEAVYMAXic} = M_{LIGHTic} + H_{CARBONi} \quad (16)$$

We assumed that the proportion of oxygen atoms in DNA that were derived from $H_2{}^{18}O$ was less than one and was equal to *U* (estimated to be 0.327 for *E. coli* in pure culture; see above). Therefore, for the ^{18}O treatment we estimated the theoretical molecular weight of newly synthesized DNA for taxon *i* as:

$$M_{HEAVYic} = M_{LIGHTic} + \left(2U \cdot H_{OXYGEN}\right) \quad (17)$$

Rearranging equation 15, we solved for the number of newly synthesized, labeled 16S copies in the heavy (^{18}O or ^{13}C) treatment:

$$Q_{HEAVYic} = Q_{LIGHTic} \cdot \left(\frac{M_{LABic} - M_{LIGHTic}}{M_{HEAVYic} - M_{LABic}} \right) \quad (18)$$

We then applied an exponential model for population growth,

$$N_d = N_0 e^{g_{ic} d} \tag{19}$$

where N_d is the number of 16S copies at time d and N_0 is the number of 16S copies at time 0. We assumed that the number of 16S copies is proportional to the number of cells. The number of 16S copies at time d is the sum of the number of light (^{16}O or ^{12}C) copies and the number of heavy (^{18}O or ^{13}C) copies:

$$N_d = Q_{ic} = Q_{LIGHTic} + Q_{HEAVYic} \tag{20}$$

Substituting the right-hand side of equation 18 into equation 20 resulted in:

$$N_d = Q_{LIGHTic} + Q_{LIGHTic} \cdot \left(\frac{M_{LABic} - M_{LIGHTic}}{M_{HEAVYic} - M_{LABic}} \right) \tag{21}$$

And rearranging yielded:

$$N_d = Q_{LIGHTic} \cdot \left(\frac{M_{HEAVYic} - M_{LIGHTic}}{M_{HEAVYic} - M_{LABic}} \right) \tag{22}$$

We assumed no microbial turnover during the incubation period, so

$$Q_{LIGHTic} = N_0 \tag{23}$$

Substituting equation 22 into equation 19 resulted in:

$$e^{g_{ic} d} = \frac{M_{HEAVYic} - M_{LIGHTic}}{M_{HEAVYic} - M_{LABic}} \tag{24}$$

We then solved for the intrinsic rate of increase:

$$g_{ic} = \frac{\ln\left(\frac{M_{HEAVYic} - M_{LIGHTic}}{M_{HEAVYic} - M_{LABic}} \right)}{d} \tag{25}$$

Modeling microbial production

To estimate standing stock biomass for each taxon, we calculated the mean number of 16S copies per gram of soil across all replicates for the heavy (^{18}O or ^{13}C) and light (^{16}O or ^{12}C) isotope additions and assumed six 16S copies in each cell and 0.1pg C cell^{-1}. We estimated production (i.e., the flux of carbon into biomass) as the product of the intrinsic rate of increase and standing stock biomass for each taxon:

$$F_{ic} = g_{ic} \cdot \frac{L}{P} \cdot \left(\frac{\sum_{j=1}^{J} \frac{y_{i1j} v}{S_{1j}} + \sum_{j=1}^{J} \frac{y_{i2j} v}{S_{2j}}}{2J} \right) \quad (26)$$

where $t = 1$ and $t = 2$ refer to the light (^{16}O or ^{12}C) and heavy (^{18}O or ^{13}C) experimental treatments, respectively. The mass of soil (S_{tj}) associated with the DNA in each replicate tube was calculated as:

$$S_{tj} = \frac{b_{tj}}{a_{tj}} \quad (27)$$

Program Manager:

Joseph R. Graber

Joseph.Graber@science.doe.gov

301-903-1239

Aanderud ZT, Jones SE, Fierer N, Lennon JT. 2015. Resuscitation of the rare boisphere contributes to pulses of ecosystem activity. *Frontiers in Microbiology* **6**.

Amann RI, Ludwig W, Schleifer KH. 1995. Phylogenetic Identification and in situ Detection of Individual Microbial Cells without Cultivation. *Microbiological Reviews* **59**(1): 143-169.

Amelung W, Brodowski S, Sandhage-Hofmann A, Bol R 2008. COMBINING BIOMARKER WITH STABLE ISOTOPE ANALYSES FOR ASSESSING THE TRANSFORMATION AND TURNOVER OF SOIL ORGANIC MATTER. In: Sparks DL ed. *Advances in Agronomy, Vol 100*, 155-250.

Behrens S, Losekann T, Pett-Ridge J, Weber PK, Ng WO, Stevenson BS, Hutcheon ID, Relman DA, Spormann AM. 2008. Linking microbial phylogeny to metabolic activity at the single-cell level by using enhanced element labeling-catalyzed reporter deposition fluorescence in situ hybridization (EL-FISH) and NanoSIMS. *Applied and Environmental Microbiology* **74**(10): 3143-3150.

Blomberg SP, Garland T, Ives AR. 2003. Testing for phylogenetic signal in comparative data: behavioral traits are more labile. *Evolution* **57**(4): 717-745.

Brown JH, Gillooly JF, Allen AP, Savage VM, West GB. 2004. Toward a metabolic theory of ecology. *Ecology* **85**(7): 1771-1789.

Buckley DH, Huangyutitham V, Hsu S-F, Nelson TA. 2007. Stable Isotope Probing with 15N Achieved by Disentangling the Effects of Genome G+C Content and Isotope Enrichmen on DNA Density. *Applied and Environmental Microbiology* **73**(10): 3189-3195.

Caporaso JG, Lauber CL, Walters WA, Berg-Lyons D, Huntley J, Fierer N, Owens SM, Betley J, Fraser L, Bauer M, Gormley N, Gilbert JA, Smith G, Knight R. 2012. Ultra-high-throughput microbial community analysis on the Illumina HiSeq and MiSeq platforms. *ISME J* **6**(8): 1621-1624.

Fierer N, Bradford MA, Jackson RB. 2007. Toward an ecological classification of soil bacteria. *Ecology* **88**(6): 1354-1364.

Goldfarb KC, Karaoz U, Hanson CA, Santee CA, Bradford MA, Treseder KK, Wallenstein MD, Brodie EL. 2011. Differential growth responses of soil bacterial taxa to carbon substrates of varying chemical recalcitrance. *Frontiers in Microbiology* **2**(May).

Hellman M, Berg J, Brandt KK, Hallin S. 2011. Survey of bromodeoxyuridine uptake among environmental bacteria and variation in uptake rates in a taxonomically diverse set of bacterial isolates. *Journal of Microbiological Methods* **86**(3): 376-378.

Hutchens E, Radajewski S, Dumont MG, McDonald IR, Murrell JC. 2004. Analysis of methanotrophic bacteria in Movile Cave by stable isotope probing. *Environmental Microbiology* **6**(2): 111-120.

Jayamani I, Cupples AM. 2015. Stable Isotope Probing and High-Throughput Sequencing Implicate Xanthomonadaceae and Rhodocyclaceae in Ethylbenzene Degradation. *Environmental Engineering Science* **32**(3): 240-249.

Kim YE, Yoon H, Kim M, Nam YJ, Kim H, Seo Y, Lee GM, Kim YJ, Kong WS, Kim JG, Seu YB. 2014. Metagenomic analysis of bacterial communities on Dokdo Island. *Journal of General and Applied Microbiology* **60**(2): 65-74.

Kramer C, Gleixner G. 2008. Soil organic matter in soil depth profiles: Distinct carbon preferences of microbial groups during carbon transformation. *Soil Biology & Biochemistry* **40**(2): 425-433.

Li XZ, Rui JP, Mao YJ, Yannarell A, Mackie R. 2014. Dynamics of the bacterial community structure in the rhizosphere of a maize cultivar. *Soil Biology & Biochemistry* **68**: 392-401.

Mau RL, Liu CM, Aziz M, Schwartz E, Dijkstra P, Marks JC, Price LB, Keim P, Hungate BA. 2014. Linking soil bacterial diversity and soil carbon stability. *The ISME Journal* **in press**.

Mayali X, Weber PK, Brodie EL, Mabery S, Hoeprich PD, Pett-Ridge J. 2012. High-throughput isotopic analysis of RNA microarrays to quantify microbial resource use. *Isme Journal* **6**(6): 1210-1221.

Mayali X, Weber PK, Pett-Ridge J. 2013. Taxon-specific C/N relative use efficiency for amino acids in an estuarine community. *FEMS microbiology ecology* **83**(2): 402-412.

Muyzer G, Dewaal EC, Uitterlinden AG. 1993. Profiling of Complex microbial-Populations by Denaturing Gradient Gel-Electrophoresis Analysis of Polymerase Chain Reaction-Amplified Genes Coding for 16S Ribosomal-RNA. *Applied and Environmental Microbiology* **59**(3): 695-700.

Nannipieri P, Ascher J, Ceccherini MT, Landi L, Pietramellara G, Renella G. 2003. Microbial diversity and soil functions. *European Journal of Soil Science* **54**(4): 655-670.

Orphan VJ, House CH, Hinrichs KU, McKeegan KD, DeLong EF. 2001. Methane-consuming archaea revealed by directly coupled isotopic and phylogenetic analysis. *Science* **293**(5529): 484-487.

Peterson BJ, Fry B. 1987. STABLE ISOTOPES IN ECOSYSTEM STUDIES. *Annual Review of Ecology and Systematics* **18**: 293-320.

Pett-Ridge J, Weber PK. 2012. NanoSIP: NanoSIMS applications for microbial biology. *Methods in molecular biology (Clifton, N.J.)* **881**: 375-408.

Pritchard JR, Schluter D. 2001. Declining interspecific competition during character displacement: Summoning the ghost of competition past. *Evolutionary Ecology Research* **3**(2): 209-220.

Radajewski S, Ineson P, Parekh NR, Murrell JC. 2000. Stable-isotope probing as a tool in microbial ecology. *Nature* **403**(6770): 646-649.

Reich PB, Walters MB, Ellsworth DS. 1997. From tropics to tundra: Global convergence in plant functioning. *Proceedings of the National Academy of Sciences of the United States of America* **94**(25): 13730-13734.

Roesch LF, Fulthorpe RR, Riva A, Casella G, Hadwin AKM, Kent AD, Daroub SH, Camargo FAO, Farmerie WG, Triplett EW. 2007. Pyrosequencing enumerates and contrasts soil microbial diversity. *Isme Journal* **1**(4): 283-290.

Rousk J, Baath E. 2011. Growth of saprotrophic fungi and bacteria in soil. *FEMS microbiology ecology* **78**(1): 17-30.

Schildkraut CL. 1962. Determinatino of Base Composition of Deoxyribonucleic Acid from its Buoyant Denstiy in CsCl. *Journal of Molecular Biology* **4**(6): 430-&.

Schimel DS. 1993. *Isotopic Techniques in Plant, Soil and Aquatic Biology: Theory and application of tracers*.

Schimel DS. 1995. Terrestrial Ecosystems and the Carbon Cycle. *Global Change Biology* **1**(1): 77-91.

Schmidt O, Horn MA, Kolb S, Drake HL. 2015. Temperature impacts differentially on the methanogenic food web of cellulose-supplemented peatland soil. *Environmental Microbiology* **17**(3).

Schwartz E, Van Horn DJ, Buelow HN, Okie JG, Gooseff MN, Barrett JE, Takacs-Vesbach CD. 2014. Characterization of growing bacterial populations in McMurdo Dry Valley soils through stable isotope probing with O-18-water. *FEMS microbiology ecology* **89**(2): 415-425.

Sharp CE, Martinez-Lorenzo A, Brady AL, Grasby SE, Dunfield PF. 2014. Methanotrophic bacteria in warm geothermal spring sediments identified using stable-isotope probing. *FEMS microbiology ecology* **90**(1).

Srivastava DS, Cadotte MW, MacDonald AAM, Marushia RG, Mirotchnick N. 2012. Phylogenetic diversity and the functioning of ecosystems. *Ecology Letters* **15**(7): 637-648.

Treonis AM, Ostle NJ, Stott AW, Primrose R, Grayston SJ, Ineson P. 2004. Identification of groups of metabolically-active rhizosphere microorganisms by stable isotope probing of PLFAs. *Soil Biology & Biochemistry* **36**(3): 533-537.

Urbach E, Vergin KL, Giovannoni SJ. 1999. Immunochemical detection and isolation of DNA from metabolically active bacteria. *Applied and Environmental Microbiology* **65**(3): 1207-1213.

West GB, Brown JH. 2005. The origin of allometric scaling laws in biology from genomes to ecosystems: towards a quantitative unifying theory of biological structure and organization. *Journal of Experimental Biology* **208**(9): 1575-1592.